Direct Measurement of the Carbon Dioxide-Induced Glass Transition Depression in a Family of Substituted Polycarbonates

TAPAN BANERJEE,[1] G. GLENN LIPSCOMB[2]

[1] 697 Rhodes Hall (ML 171), Chemical Engineering Department, University of Cincinnati, Cincinnati, Ohio 45221-0171

[2] 2801 W. Bancroft, Chemical Engineering Department, University of Toledo, Toledo, OH 43606-3390

Received 20 January 1997; accepted 30 October 1997

ABSTRACT: We present a method for the direct measurement of the glass transition temperature of compressed gas–polymer systems. The technique utilizes a Setaram C80D microcalorimeter equipped with high-pressure cells. Pressurizing the cells and running in scanning mode allows direct determination of the glass transition temperature. To validate the method, T_g measurements of the CO_2–poly(methyl methacrylate) system as a function of gas phase pressure were made. The results compare favorably with literature values. However, the effects of foaming appear to interfere with T_g measurement at the highest gas pressures. The CO_2-induced T_g depression of a series of polycarbonates was also measured. The magnitude of the T_g depression increases with decreasing glass transition temperature, reflecting an increase in intrinsic chain mobility, as evidenced by the glass transition temperature. The data correlate well with the Chow model. © 1998 John Wiley & Sons, Inc. J Appl Polym Sci 68: 1441–1449, 1998

Key words: glass transition; plasticization; polycarbonate; carbon dioxide

INTRODUCTION

Gas sorption in glassy polymeric materials is a technologically important phenomenon. Membrane separation processes utilize differences in sorption and diffusion to effect a separation.[1] Moreover, solubility and diffusivity in glassy polymeric materials can be quite sensitive to the concentration of the sorbed species, especially highly soluble species such as CO_2. Such plasticization effects can be detrimental in a separation process.[1,2]

Conditioning a glassy polymer by exposing it to a highly soluble penetrant (for example, CO_2) at high activity (for example, high pressure) and then removing the penetrant can increase the permeability of other species.[3–5] Transport rates can increase even if the CO_2 is not removed. This effect has been exploited to help extract impurities from[6–8] and introduce additives in[9] polymeric materials.

One can also produce novel glassy structures through processes that utilize gas sorption to assist processing. Examples include the production of microcellular foams,[10,11] thin films and fibers,[12,13] and microspheres.[14]

The effect of gas sorption on the glass transition temperature (T_g) is of great concern in these applications. One typically either wants to remain below the glass transition (as in membrane separation processes) or pass through the transition in

Correspondence to: G. Lipscomb (glenn.lipscomb@utoledo.edu).

Contract grant sponsor: ACS, Petroleum Research Fund; contract grant number: PRF 23536-G7; contract grant sponsor: National Science Foundation; contract grant number: CTS-9011207.

Journal of Applied Polymer Science, Vol. 68, 1441–1449 (1998)
 CCC 0021-8995/98/091441-09

a controlled fashion (as in the process to produce microcellular foams).

Numerous experimental techniques are available to determine the glass transition in the absence of sorption.[15] The need to contact a high-pressure gas phase with the sample makes glass transition measurements in the presence of gas sorption problematic. A variety of experimental techniques that address this problem are available in the literature. These techniques differ not only in the material property that is measured but how the gas contacts the polymer; *in situ* methods permit gas–polymer contact during the measurement while *ex situ* methods use preequilibrated samples under ambient conditions; thus, gas desorption occurs during the measurement.

Kamiya et al.[16] and Wissinger and Paulaitis[17] reported the use of dilatometry to measure T_g *in situ*. The discontinuity in the slope of the specific volume–temperature curve, however, is difficult to precisely locate. Complementary solubility data also show a subtle discontinuity.[18]

Kamiya et al.[19] and Goel and Beckman[20] used dielectric relaxation spectroscopy to measure T_g *in situ*. Measured T_gs are slightly lower than those obtained from solubility data.

A number of investigators have reported *in situ* creep compliance measurements. Wang et al.[21] described the first results, but Wissinger and Paulaitis[22] proposed improvements to the data analysis and emphasized the relationship between T_g or P_g (the gas pressure at which a glass–rubber transition takes place at constant temperature) and the gas concentration while Johnston and coworkers[23,24] expanded the range of conditions over which measurements are made to demonstrate retrograde vitrification (the occurrence of a rubber to glass transition with increasing temperature). Fried et al.[25] also reported T_g from mechanical property measurements but using samples *ex situ*.

Wonders and Paul[26] reported *in situ* T_g measurements using a modified differential thermal analyzer. Experimental difficulties led to the development of an *ex situ* differential scanning calorimetric method by Chiou et al.[27] that has been subsequently utilized by Sanders.[2] Hachisuka et al.[28] discussed a modification of this method that equilibrates the sample with CO_2 prior to the experiment by placing both the sample and solid CO_2 (dry ice) in the pan used for measurement.

Handa and coworkers[29,30] recently described the use of a high-pressure differential scanning calorimeter (DSC) for *in situ* T_g measurements. Measurements are reported using both a modified Setaram BT calorimeter and a TA Instruments 2910 DSC equipped with the high-pressure (Pressure DSC) PDSC cell. The measurements agree well with T_g values obtained by other methods.

Numerous theoretical analyses of T_g depression are available in the literature. All use lattice fluid theory (see, for example, Sanchez and Lacombe,[31] and Panayiotou and Vera[32]) to describe gas–polymer thermodynamics and the Gibbs–DiMarzio criterion[33,34] (the entropy of the gas–polymer mixture is zero) for the glass transition. The analysis of Chow[35] was the first to appear and is the easiest to use. The analyses of Wissinger and Paulaitis[36] and Condo et al.[37] account for more molecular detail but also require more detailed experimental data to evaluate.

We report here an *in situ* method similar to that of Handa and coworkers. The experiments utilize a Setaram C80 DSC equipped with high-pressure cells. T_g measurements of the CO_2–poly(methyl methacrylate) (PMMA) system compare favorably with reported literature values. However, we see evidence of gas foaming that limits the ability to determine T_g at the highest gas phase pressures. Additionally, we examine the effect of sample dimensions and heating rate.

Measurements for commercially important CO_2–polycarbonate (PC), CO_2–tetramethyl polycarbonate (TMPC), CO_2–tetrachloro polycarbonate (TCPC), and CO_2–tetrabromo polycarbonate (TBPC) systems are also reported. The results indicate that T_g depression decreases with decreasing intrinsic chain mobility at a fixed gas concentration. Results for PC are described well by the Chow model.

EXPERIMENTAL

PC was obtained from the Aldrich Chemical Company (Milwaukee, WI). All of the substituted polycarbonates were generously provided by the Dow Chemical Company (Midland, MI). PMMA was obtained from Scientific Polymer Products, Inc. (Ontario, NY)

All of the polymeric materials are highly soluble in methylene chloride (Fischer, Pittsburgh, PA). To prepare film samples, 10% by weight solutions of each were prepared. After casting the solution on a glass plate using a casting knife (Gardner, Pompano Beach, FL), films were dried at atmospheric conditions for 10–24 h. Subsequently, films were placed in a vacuum at room tempera-

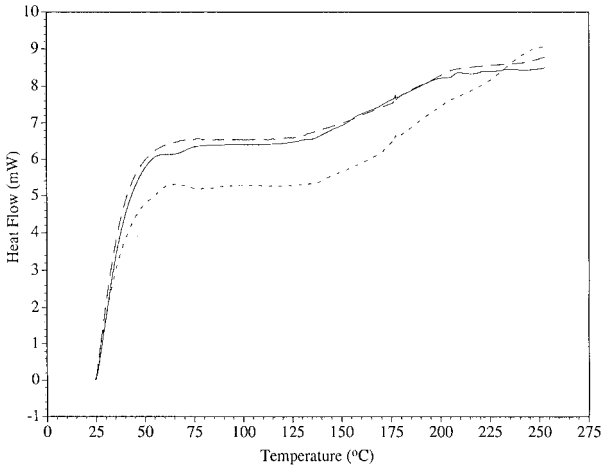

Figure 1 Heat flow without a sample at various CO_2 pressures: solid, 0 atm; short dash, 25 atm; long dash, 35 atm.

ture for 24 h and annealed at ~ 20°C below T_g for 3 days. DSC scans showed no signs of residual solvent or crystallinity. Final film thickness was ~ 10–15 μm.

T_g measurements were performed using a Setaram C80D microcalorimeter equipped with high-pressure cells. A detailed description of the apparatus is available in the literature.[38]

The experimental procedure consists of the following steps.

1. Place film directly in sample cell; leave the reference cell empty. Sample masses ranging from 0.1 to 0.5 g were used.
2. Evacuate both cells and establish the thermal baseline.
3. Introduce gas and hold at initial temperature for 2–4 h until the thermal baseline is reestablished.
4. Ramp the temperature from the initial temperature to T_g + 20°C at a rate of 1°C/min.
5. The glass transition is taken as the point at which 50% of the change in heat flow occurs.

We report the first scan only (except where noted) to avoid complications due to CO_2 conditioning. Additionally, checks of the temperature calibration using gallium (melting point of 29.8°C) and indium (melting point of 156.9°C) indicate temperature measurement error is approximately 0.5°C.[38]

RESULTS AND DISCUSSION

Results obtained with empty cells at various gas pressures are shown in Figure 1. Note that the heat flow does not reach a baseline until approximately 20 min (after the temperature increases 20°C) after the start of the temperature ramp. After that, the baseline remains flat until a temperature of ~ 150°C, after which the baseline increases gradually by 2 mW over the next 60°C and then flattens out. This suggests the cells remain well sealed and that changes in the baseline with heating should not interfere with T_g identification (no T_g like baseline changes occur).

Representative results for PMMA at low CO_2 pressures are shown in Figure 2. After an initial transient of equal length to that observed for the empty cells, a baseline is established, and then a glass transition is observed. After the experiment, the films placed in the sample cell readily separated and showed no signs of foaming.

Results obtained at intermediate pressures are shown in Figure 3. At 25 atm, the initial transient is greater than at lower pressures, and a baseline prior to the glass transition is not established. However, a glass transition is readily apparent, and, after the transition, a baseline is established.

Upon increasing the pressure to 30 and 35 atm, the heat flow switches directions at the lower temperatures and passes through a minimum and then a maximum before an apparent glass transition occurs. We attribute this endothermic minimum to rapid CO_2 loss through the formation of small gas bubbles (a microfoam).

Macroscopic foaming is apparent for large samples, with volumes greater than approximately 0.5 cm^3, and the film samples weld together into one large mass. Macroscopic foaming is not apparent, however, if the sample volume is reduced.

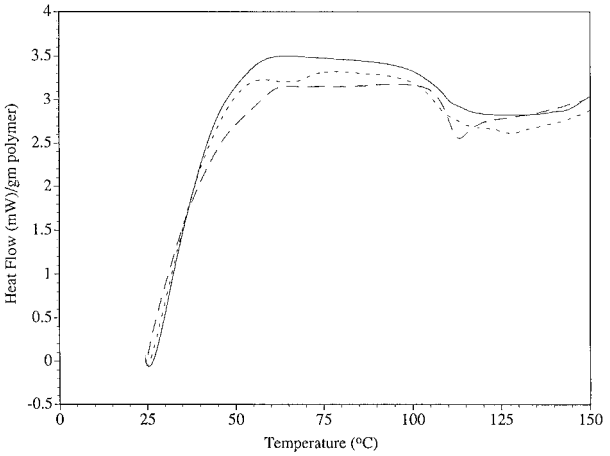

Figure 2 Heat flow for PMMA at low CO_2 pressures: solid, 0 atm; short dash, 1 atm; long dash, 5 atm.

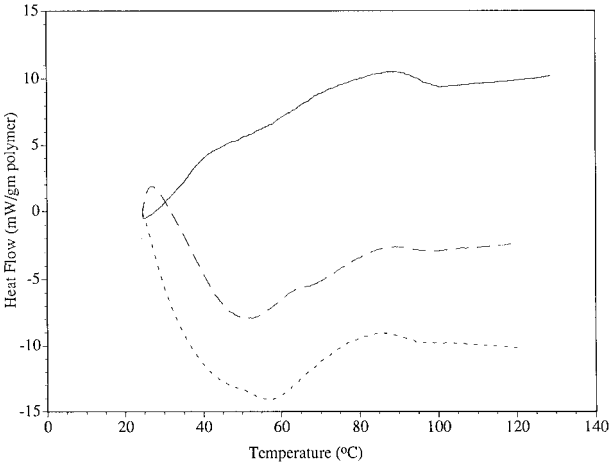

Figure 3 Heat flow for PMMA at intermediate CO_2 pressures: solid, 25 atm; short dash, 30 atm; long dash, 35 atm.

The films still weld together, but any bubbles that form are eliminated during the experiment.

The supersaturation driving force for bubble formation arises from the concentration lag relative to the equilibrium concentration for the given pressure and temperature. To estimate the magnitude of the concentration lag, we will use the solution to the unsteady mass transfer problem into a finite slab.[39] After a step change in surface concentration (due to an instantaneous temperature change and the associated change in gas solubility), the concentration field in the center of the slab will reach approximately 90% of its final value after a time t_{90} has elapsed where t_{90} is given by

$$t_{90} = \frac{l^2}{4D} \qquad (1)$$

where l is the film thickness and D is the diffusion coefficient. Since thermal diffusivities are several orders of magnitude larger than mass diffusivities for the systems considered here, thermal changes occur virtually instantaneously relative to mass changes.

For a 15-μm film and diffusivity of 1E-9 cm^2/s, one calculates t_{90} = 9.4 min. During this time, the temperature will increase 9.4°C. Thus, some gas supersaturation will occur during the experiment, and the potential for foaming exists. Additionally, the magnitude of supersaturation would increase if films welded together to effectively increase film thickness; we believe this is why larger sample volumes show macroscopic foaming.

The apparent foaming at lower temperatures and presence of a glass transition at higher temperatures suggests the sample is close to a rubber–glass transition (retrograde vitrification) at the initial temperature of 25°C, as illustrated in Figure 4. The supersaturation resulting from concentration lag makes the effective gas pressure slightly larger than the experimental pressure. This moves the sample toward the glass transition curve. Upon heating, the sample will move away from the glass transition curve but must encounter it again if heating is continued.

Experiments with thicker samples (thicknesses of 1000 μm) clearly showed macroscopic foaming, due to the increased concentration lag, at pressures lower than 25 atm. Clearly, sample thickness is an important variable in DSC experiments, and one should use samples with the shortest diffusion length scale (for example, sample thickness) possible.

Results obtained at the highest experimental pressures are shown in Figure 5. The heat flow passes through an endothermic minimum, but no evidence of a glass transition exists afterwards. This suggests the sample remains rubbery over the temperature range of the experiment. The transition from the behavior observed in Figure

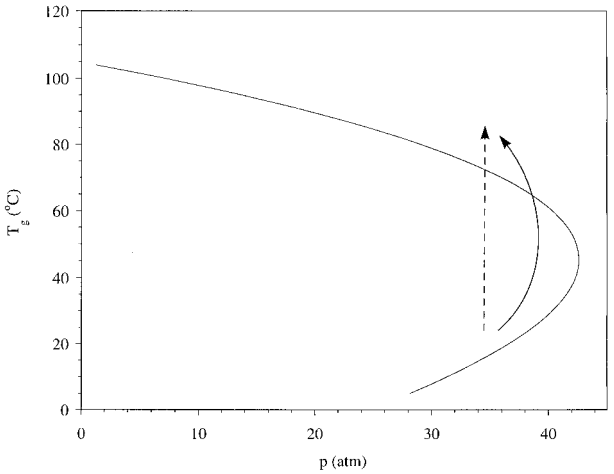

Figure 4 Effect of concentration lag on glass transition measurements. The solid line represents PMMA glass transition temperature as a function of CO_2 pressure.[37] Ideally, the sample traverses the temperature–pressure path indicated by the dashed line. However, concentration lag increases gas concentration at each point along this path relative to the equilibrium value for the given gas phase pressure and temperature. The solid line represents the temperature–pressure path based on the effective pressure: the pressure required to give the actual gas concentration.

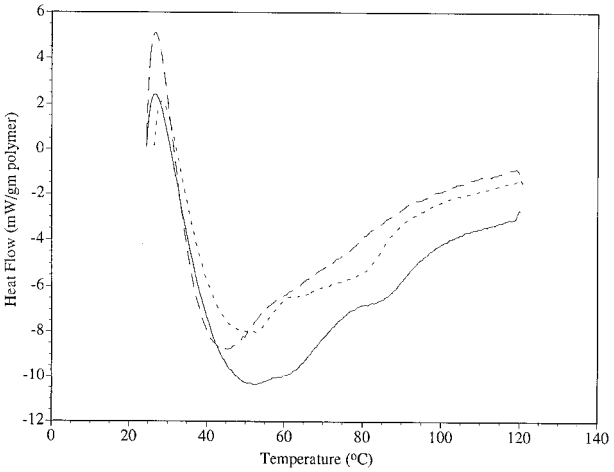

Figure 5 Heat flow for PMMA at high CO_2 pressures: solid, 45 atm; short dash, 51 atm; long dash, 58 atm.

3 to that found in Figure 5 occurs at approximately 40 atm.

For comparison purposes, the thermal changes for a poly(dimethyl siloxane) (PDMS) sample[38] are shown in Figure 6. PDMS remains rubbery over the range of experimental conditions used. These curves are similar in shape to those obtained for PMMA at pressures greater than 40 atm, supporting our contention that PMMA is rubbery at those conditions. Note that changes in the curve are relatively small despite the fact that the pressure increases from 0 to 50 atm, and the slight minimum observed at 50 atm suggests that some foaming is occurring.

The T_g values obtained from these experiments

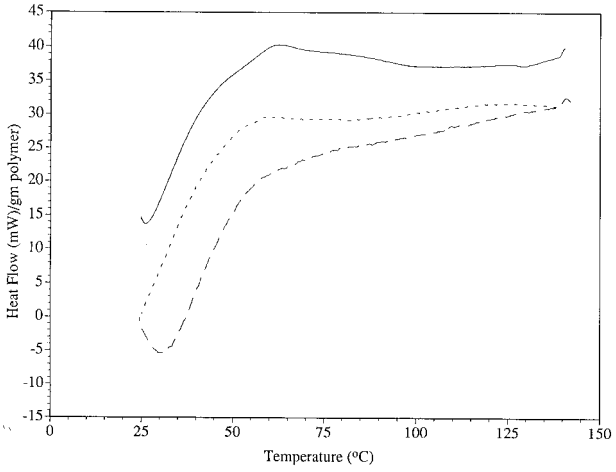

Figure 6 Heat flow for PDMS at various CO_2 pressures: solid, 0 atm; short dash, 25 atm; long dash, 50 atm.

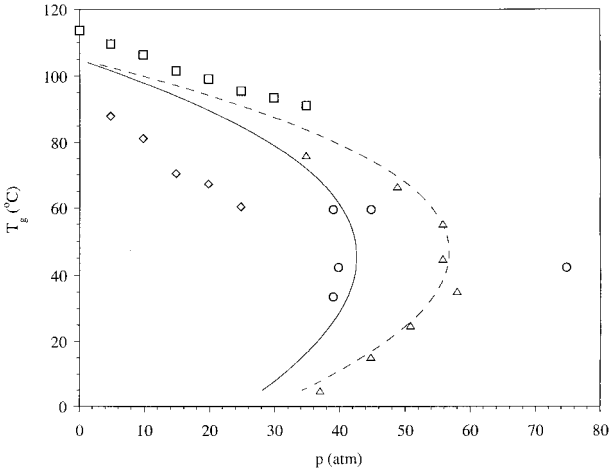

Figure 7 PMMA glass transition temperature as a function of CO_2 gas phase pressure: this work, squares; Wissinger and Paulaitis,[22] circles; Condo and Johnston,[23,24] triangles; Chiou et al.,[27] diamonds. The solid line is drawn through the data of Wissinger and Paulaitis[22] to aid the reader while the dashed line represents the glass transition temperature predicted by Condo et al.[37]

are plotted as a function of gas pressure in Figure 7 along with available literature data. Overall the agreement is good. The decrease in T_g with increasing gas pressure is comparable to that observed in the literature. The maximum pressure at which a glass transition is observed falls in between the data of Wissinger and Paulaitis[22] and Condo and Johnston.[23,24] However, since we did not possess the capability to cool the calorimeter below ambient temperature, we were unable to observe retrograde vitrification as reported by the latter authors.

Figure 8 shows the variation of the change in heat capacity at the glass–rubber transition as a function of gas pressure. The data are nearly linear as indicated by the results of a linear regression also shown in Figure 8. If the glassy state disappears as gas pressure increases, one would expect ΔC_p to decrease with increasing pressure as observed and extrapolating ΔC_p to zero should give a good estimate of the maximum pressure at which PMMA is a glass. The value of 35 atm agrees well with the value estimated from Figures 3 and 5.

The T_g depression found for the substituted polycarbonate polymers is shown in Figure 9. Specific values for the zero-pressure T_g of each polymer are given in Table I. Note that for these polymers, the CO_2 diffusivity is greater than 1E-8 cm^2/s, so the estimates of the concentration and ther-

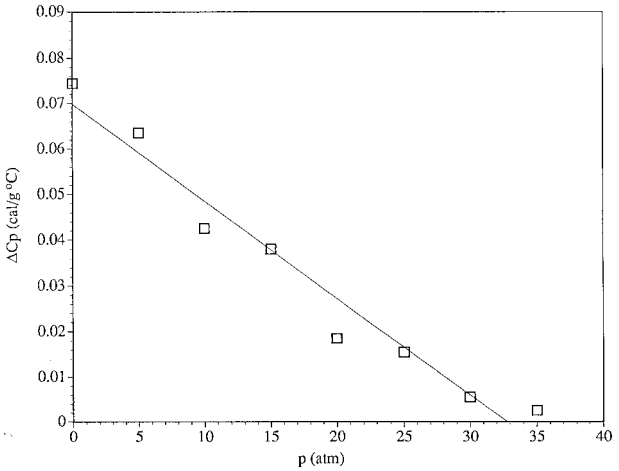

Figure 8 Variation in ΔC_p with gas phase pressure. The solid line shows the results of a linear regression of the data.

mal lag obtained from eq. (1) become ~ 1 min and ~ 1°C, respectively.

The T_gs observed under vacuum agree well with reported literature values, as indicated in Table I. The rate of change of T_g with pressure decreases as the zero pressure T_g of the polymer increases. The glass transition depression decreases in magnitude as the intrinsic mobility of the polymer decreases, even though gas solubility is higher in the higher T_g materials. This suggests changes in intrinsic chain mobility have a greater influence than gas solubility on T_g.

We also examined the effects of conditioning on T_g depression for PC. The glass transition temperature of samples conditioned for 24 h at CO_2 pressures of 300, 600, and 800 psig prior to a DSC scan at the same pressure are given in Table II. Conditioning appears to have no effect on the glass transition for pressures up to 600 psig; T_g varies by less than 3%. However, conditioning at 800 psig leads to a reduction in T_g of ~ 14%.

This decrease in glass transition temperature would be consistent with an increase in gas solubility. It is well known that, after conditioning at a high pressure, gas solubilities at lower pressures are greater than in the absence of conditioning. We hypothesize that a similar, but much less pronounced, effect may occur with increasing temperature. After conditioning at a lower temperature, solubility is higher at higher temperatures than in the absence of conditioning.

The effect of conditioning in both cases is to open up the glassy matrix. As gas is removed by either depressurizing or heating, the matrix does not relax (contract), over experimental time scales, to the same state as an unconditioned sample. Hence, additional excess free volume is available for sorption and solubility increases.

If solubility and concentration are higher at higher temperatures, one would expect to pass through the glass transition at a lower temperature as observed experimentally. Increased chain mobility at higher temperatures, though, will re-

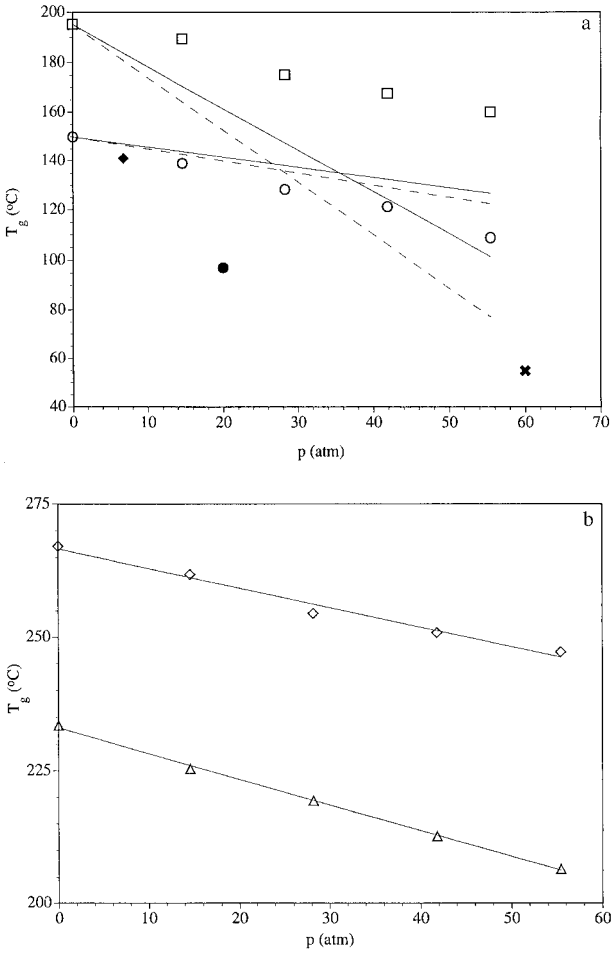

Figure 9 (a) Glass transition temperature as a function of pressure for PC (open circles) and TMPC (open squares). The lines drawn through the data represent the predictions of the Chow model[35] for $z = 1$ (solid) and $z = 2$ (dashed). The filled symbols represent other data available in the literature for PC: filled diamond, Wonders and Paul[26]; filled circle, Chiou et al.[27]; filled cross, Hachisuka et al.[28] (b) Glass transition temperature as a function of pressure for TCPC (triangles) and TBPC (diamonds). The solid lines drawn through the TCPC and TBPC data serve only as a guide for the reader.

Table I Zero-Pressure T_g Values

Material	Zero-Pressure T_g (°C)	Literature T_g[42] (°C)
PC	150	150
TMPC	195	193
TCPC	233	230
TBPC	267	263

duce the magnitude of any solubility increase as excess free volume is more easily eliminated. If mobility increases fast enough, one would see little change in T_g. Therefore, the effect of conditioning on T_g will depend on the relative rates at which gas concentration changes and chain mobility increases. For PC, the net effect is little change in T_g, except at the highest conditioning pressures, where the difference between the conditioning temperature and T_g is smallest and the time for chain relaxation is shortest.

One would also expect conditioning-induced changes to be greater at higher pressures if the glassy state does not exist beyond some maximum gas pressure as observed for the CO_2–PMMA system. The strong dependence of T_g on concentration in the vicinity of this pressure (a large decrease in T_g with a small increase in solubility) would lead to more pronounced changes.

We will use the theoretical analysis of Chow[35] to provide theoretical estimates of T_g depression. Chow derived the following expression for the T_g of a diluent–polymer mixture:

$$\ln\left[\frac{T_g}{T_{g0}}\right] = \beta[(1-\theta)\ln(1-\theta) + \theta \ln \theta] \quad (2)$$

where T_{g0} is the glass transition temperature of the diluent free polymer. The parameters β and θ are given by

$$\beta = \frac{zR}{M_p \Delta C_p} \quad (3)$$

and

$$\theta = \frac{M_p}{zM_d}\frac{\omega}{1-\omega} \quad (4)$$

where z is the coordination number, R is the gas constant, M_p is the polymer repeat unit molecular weight, M_d is the diluent molecular weight, ΔC_p is the change in polymer heat capacity at the glass transition, and ω is the diluent weight fraction. Values for these parameters are either available in the literature or can be measured in independent experiments, except for z, which most commonly is taken as either 1 or 2.[27,35]

Of the substituted polycarbonates examined here, literature values for the parameters in eq. (2), especially the temperature-dependent solubility data, are available only for PC and TMPC. Table III gives the values used for each parameter; solubility data was taken from the literature.[41]

Figure 9 compares the predicted T_g depression to the experimental results. Despite its theoretical limitations, the Chow theory provides remarkably good estimates of T_g depression over a broad concentration range for PC and TMPC. We find that a z value of 2 gives better results for PC while a z value of 1 gives better results for TMPC.

CONCLUSIONS

We present a procedure for the direct measurement of the gas-induced glass transition depression of glassy polymeric materials. The experiments utilize a commercial high-pressure microcalorimeter operated in a DSC mode. To obtain unambiguous results, one must choose sample dimensions such that diffusion time scales are smaller than experimental heating time scales. Otherwise, concentration lag interferes with an accurate measurement of the concentration dependence of T_g.

Measurements of the CO_2-induced glass transition depression of PMMA are in good agreement with previous work. The results suggest sample foaming during the experiment can also interfere with T_g determination, especially for systems that exhibit retrograde vitrification.

Within a family of substituted polycarbonates,

Table II Material Parameters for PC and TMPC Used to Estimate T_g Depression from the Chow Theory

Material	z	M_p (g/mol)	ΔC_p (cal g^{-1} °C^{-1})
PC	1 and 2	254	0.0775
TMPC	1 and 2	310	0.0170

Table III Effect of Conditioning on T_g Depression in PC

Conditioning/ Experimental Pressure (psig)	Unconditioned T_g (°C)	Conditioned T_g (°C)	Percent Difference
300	134	137	+2.2
600	121	123	+1.7
800	109	94	−14

the magnitude of T_g depression decreases with increasing pure polymer T_g. Intrinsic chain mobility apparently has a greater influence on glass transition behavior than gas solubility for these systems.

Conditioning PC prior to T_g measurement has no effect for gas pressures less than 600 psig. At 800 psig, though, a $\sim$ 14% drop in T_g is observed. This behavior may be due to an increase in gas solubility imparted by conditioning. Increases in chain mobility during the T_g measurement tend to eliminate conditioning effects, but under appropriate experimental conditions, the solubility increase may be large enough to have a measurable influence on T_g.

Finally, the Chow theory of T_g depression for diluent–polymer systems provides good predictions of the experimental results for PC and TMPC. These observations, along with prior work, suggest that the Chow theory is a useful tool for evaluating the T_g sensitivity of diluent–polymer systems.

REFERENCES

1. W. S. Ho and K. K. Sirkar, Eds., *Membrane Handbook,* Van Nostrand Reinhold, New York, 1992.
2. E. S. Sanders, *J. Membr. Sci.,* **37,** 63 (1988).
3. S. M. Jordan, W. J. Koros, and G. K. Fleming, *J. Membr. Sci.,* **30,** 191 (1987).
4. S. M. Jordan, W. J. Koros, and J. K. Beasley, *J. Membr. Sci.,* **43,** 103 (1989).
5. S. M. Jordan and W. J. Koros, *J. Membr. Sci.,* **51,** 233 (1990).
6. J. J. Shim and K. P. Johnston, *AIChEJ,* **35,** 1097 (1989).
7. J. J. Shim and K. P. Johnston, *J. Phys. Chem.,* **95,** 353 (1991).
8. J. J. Shim and K. P. Johnston, *AIChEJ,* **37,** 607 (1991).
9. A. R. Berens, G. S. Huvard, R. W. Korsmeyer, and F. W. Kuning, *J. Appl. Polym. Sci.,* **46,** 231 (1992).
10. J. E. Martini-Vvedensky, N. P. Suh, and F. A. Waldman, U.S. Pat. 4,473,665, 1984.
11. V. Kumar and N. P. Suh, *Polym. Eng. Sci.,* **30,** 1323 (1990).
12. D. W. Matson, J. L. Fulton, R. C. Petersen, and R. D. Smith, *Ind. Eng. Chem. Res.,* **26,** 2298 (1987).
13. R. C. Petersen, D. W. Matson, and R. D. Smith, *Polym. Eng. Sci.,* **27,** 1693 (1987).
14. J. W. Tom and P. G. Debenedetti, *Biotechnol. Prog.,* **7,** 403 (1991).
15. J. R. Fried, *Polymer Science and Technology,* Prentice-Hall, Englewood Cliffs, NJ, 1995.
16. Y. Kamiya, K. Mizoguchi, T. Hiroshi, and Y. Naito, *J. Polym. Sci., Polym. Phys.,* **27,** 879 (1989).
17. R. G. Wissinger and M. E. Paulaitis, *J. Polym. Sci., Polym. Phys.,* **25,** 2497 (1987).
18. J. S. Chiou, Y. Maeda, and D. R. Paul, *J. Appl. Polym. Sci.,* **30,** 4019 (1985).
19. Y. Kamiya, K. Mizoguchi, and N. Yasutoshi, *J. Polym. Sci., Polym. Phys.,* **28,** 1955 (1990).
20. S. K. Goel and E. J. Beckman, *Polymer,* **34,** 1410 (1993).
21. W. V. Wang, E. J. Kramer, and W. H. Sachse, *J. Polym. Sci., Polym. Phys.,* **20,** 1371 (1982).
22. R. G. Wissinger and M. E. Paulaitis, *J. Polym. Sci., Polym. Phys.,* **29,** 631 (1991).
23. P. D. Condo and K. P. Johnston, *J. Polym. Sci., Polym. Phys.,* **32,** 523 (1994).
24. P. D. Condo and K. P. Johnston, *Macromolecules,* **25,** 6730 (1992).
25. J. R. Fried, H.-C. Liu, and C. Zhang, *J. Polym. Sci., Part C: Polym. Lett.,* **27,** 385 (1989).
26. A. G. Wonders and D. R. Paul, *J. Membr. Sci.,* **5,** 63 (1979).
27. J. S. Chiou, J. W. Barlow, and D. R. Paul, *J. Appl. Polym. Sci.,* **30,** 2633 (1985).
28. H. Hachisuka, T. Sato, T. Imai, Y. Tsujita, A. Takizawa, and T. Kinoshita, *Polym. J.,* **22,** 77 (1990).
29. Y. P. Handa, S. Capowski, and M. O'Neill, *Thermochim. Acta,* **226,** 177 (1993).
30. Y. P. Handa, S. Lampron, and M. L. O'Neill, *J. Polym. Sci., Polym. Phys.,* **32,** 2549 (1994).
31. I. C. Sanchez and R. H. Lacombe, *Macromolecules,* **11,** 1145 (1978).

32. C. Panayiotou and J. H. Vera, *Polym. J.,* **14,** 681 (1982).
33. J. H. Gibbs and E. A. DiMarzio, *J. Chem. Phys.,* **28,** 373 (1958).
34. E. A. DiMarzio and J. H. Gibbs, *J. Polym. Sci., Part A,* **1,** 1417 (1963).
35. T. S. Chow, *Macromolecules,* **13,** 362 (1980).
36. R. G. Wissinger and M. E. Paulaitis, *Ind. Eng. Chem. Res.,* **30,** 842 (1991).
37. P. D. Condo, I. C. Sanchez, C. G. Panayiotou, and K. P. Johnston, *Macromolecules,* **25,** 6119 (1992).
38. T. Banerjee, M. Chhajer, and G. G. Lipscomb, *Macromolecules,* **28,** 8563 (1995).
39. R. B. Bird, W. E. Stewart, and E. N. Lightfoot, *Transport Phenomena,* Wiley, New York, 1960.
40. D. J. Plazek and K. L. Ngai, in *Physical Properties of Polymers Handbook,* J. E. Mark, Ed., American Institute of Physics, Woodbury, NY, 1996.
41. L. M. Costello and W. J. Koros, *J. Polym. Sci., Polym. Phys.,* **32,** 701 (1994).
42. N. Muruganandam, W. J. Koros, and D. R. Paul, *J. Polym. Sci., Polym. Phys.,* **25,** 1999 (1987).